12

Distance Estimation based on 802.11 RTS/CTS Mechanism for Indoor Localization

Alfonso Bahillo, Patricia Fernández, Javier Prieto, Santiago Mazuelas, Rubén M. Lorenzo and Evaristo J. Abril
University of Valladolid
Spain

1. Introduction

Intense research work is being carried out to design and build localization schemes that can operate in indoor environments where satellite signals typically fail. The objective is to achieve a degree of accuracy, reliability and cost in indoor environments comparable to the well-known Global Navigation Satellite Systems (GNSS) in open areas. These challenging problems are being faced today to fulfill commercial, public safety and military applications (Gustafsson & Gunnarson, 2005; Pahlavan & Krishnamurthy, 2002). In commercial applications for residential and nursing homes there is an increasing need to track people with special needs, such as children and elderly people who are out of regular visual supervision, navigate the blind, and find specific items in warehouses. For public safety and military applications, indoor localization schemes are needed to track inmates in prisons or navigate police officers, fire fighters and soldiers to complete their missions inside buildings.
Among the many indoor technological possibilities that have been considered for indoor localization such as infrared, ultrasonic and artificial vision, radiofrequency based schemes predominate today due to their availability, low-cost and coverage range. Currently, few radiofrequency infrastructures that operate inside buildings are as extensively deployed and used as 802.11. Nowadays, many buildings such as shopping malls, museums, hospitals, airports, etc. are equipped with 802.11 access points (APs). Therefore, it may be practical to use these APs to determine user location in these indoor environments.
Whichever indoor wireless technology is involved, the purpose of localization schemes is to find the unknown position of a mobile station (MS) given a set of measurements called localization metrics. These metrics could be the measured time-of-arrival (TOA) (Golden & Bateman, 2007), angle-of-arrival (AOA) (Seow & Tan, 2008) or received-signal-strength (RSS) (Mazuelas et al., 2009) of the MS's signal at the reference devices or APs. Techniques based on RSS require channel modeling and they are not flexible because they present high variability to environmental changes; even though building and updating a RSS database is much easier in indoor environments than in wide urban areas. The major drawback of pattern recognition techniques still lies in substantial efforts needed in generation and maintenance of the RSS database in view of the fact that the working environment changes constantly. Techniques based on TOA need time synchronization between wireless nodes; and techniques based on AOA require specialized antennas. Furthermore, it is important to point out that as the

measurements of metrics become less reliable, the complexity of the positioning algorithm increases.

In this chapter, the performance of the 802.11 wireless networks for indoor localization is based on the time delay localization metric through round-trip time (RTT) measurements. The challenge is to develop an infrastructure that is inexpensive to design and deploy, complies with frequency regulations, and provides a comprehensive coverage for accurate ranging. RTT is used instead of TOA to avoid the need for time synchronization between wireless nodes. Furthermore, due to the use of an 802.11 infrastructure, the location capabilities will be an added value to the existing connectivity ones. The main characteristic that makes the RTT measurements possible in any 802.11 wireless network is the common protection mechanisms to fully reserve a shared medium, Request To Send/Clear To Send (RTS/CTS) handshake (Bahillo et al., 2009). Therefore, the RTT measurements are obtained by measuring the latency of a series of layer two CTS frames sent by and in response to a corresponding series of RTS frames initiated by the MS that is going to be located. The measuring system is integrated in a Printed Circuit Board (PCB), which is used as additional hardware to the 802.11 adapter from which appropriate signals, such as transmission and receiver pulses of exchange frames, are extracted to quantify the RTT.

The results of RTT measurements in different scenarios are qualitatively consistent because, as it was expected, the delay profile observed shifts as the actual distance between wireless nodes in line-of-sight (LOS) increases following a linear shape. The coefficient of determination is used to measure how much of the original uncertainty in the RTT measurements is explained by the linear model.

Unfortunately, the assumption that a direct sight exists between two wireless nodes in an indoor environment is an oversimplification of reality, where the obstacles usually block the direct path. Known as non-line-of-sight (NLOS), several techniques have emerge to overcome this problem. They can be broadly classified in two groups, techniques which attempt to minimize the contribution of NLOS multipaths (Chen, 1999) or techniques which focus on the identification of NLOS reference devices and discard them for localization (Cong & Zhuang, 2005). However, their reliability remains questionable in an indoor environment with abundant scatterers where almost all reference devices will be in NLOS. In this chapter the PNMC (Prior NLOS Measurements Correction) technique is used to correct the NLOS effect from distance estimates (Mazuelas et al., 2008). This technique manages to introduce the information that actually resides in the NLOS measurements in the localization process.

The chapter is organized as follows. Section 2 presents a method to quantify the time delay between two wireless nodes and proposes a PCB as a measuring system. Section 3 analyzes the best statistical estimator of the time delay assuming a linear regression model to relate that estimator with the actual distance between two wireless nodes in LOS. Section 4 describes the mitigation of the severe NLOS effect on those distance estimates using the PNMC method. Section 5 evaluates the performance of the distance estimation technique in a rich multipath indoor environment, and Section 6 summarizes the main achievements.

2. Time delay quantification

The TOA-based systems measure distance based on an estimate of signal propagation delay between a transmitter and a receiver since, in free space or air, radio signals travel at the constant speed of light. The TOA can be measured by either measuring the phase of received narrowband carrier signal or directly measuring the arrival time of a wideband narrow pulse. However, the challenge for this chapter is to develop a distance estimation system

that is inexpensive to design and deploy, complies with 802.11 regulations, and provides a comprehensive coverage for accurate ranging.
That is why in this chapter the performance of the 802.11 wireless networks for indoor localization is based on the time delay localization metric through RTT measurements. By using RTT the need for time synchronization between wireless nodes is avoided which would entail a major increase in the complexity of the location scheme development. Furthermore, due to the use of an 802.11 infrastructure, the location capabilities will be an added value to the existing connectivity ones.
The main characteristic that makes the RTT measurements possible in a 802.11 wireless network is the common protection mechanism to reserve a shared medium, RTS/CTS handshake (Gast, 2002).

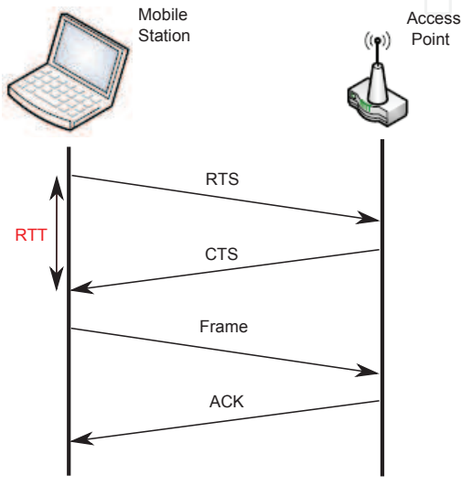

Fig. 1. RTS/CTS handshake.

In wireless communication networks, medium access control (MAC) schemes are used to manage all nodes' access to the shared wireless medium. Due to the randomness of packet arrivals and local competition, it is difficult to completely eliminate packet collisions. Since data packet collisions are costly, researchers proposed to use the RTS/CTS dialogue to reserve the right to channel usage. Assuming a ready node has a frame to send, if it has the RTS/CTS technique activated (see Fig. 1), it initiates the process by sending an RTS frame. The RTS frame serves several purposes; in addition to reserving the radio link for transmission, it silences any station that hear it. If the target station receives an RTS, it responds with a CTS. Like the RTS frame, the CTS frame silences stations in the immediate vicinity. Once RTS/CTS exchange is complete, the mobile station can transmit its frames without worry of interference from any hidden nodes. Hidden nodes beyond the range of the sending station are silenced by the CTS from the receiver. With the use of the RTS/CTS dialogue, it is less likely that data packets will suffer collisions.
Therefore, the RTS/CTS handshake is used to quantify the RTT by measuring the latency of a series of layer two CTS frames sent by and in response to a corresponding series of RTS frames initiated by the MS that is going to be located. The same as acknowledgement (ACK), CTS are considered in the AP the highest priority frames, therefore, the minimum elapsed time in the AP is guarantee when processing these sort of frames.

2.1 Printed circuit board design

In order to quantify the RTT of the RTS/CTS two-frame exchange 802.11 mechanism, appropriate signals from within the WLAN adapter chip set must be selected and accessed by the measuring system. The aim is to extract both transmission pulses and receiver signals in such a way that the RTS frame can be used as the trigger to start the measuring system that would be stopped by the corresponding CTS frame.

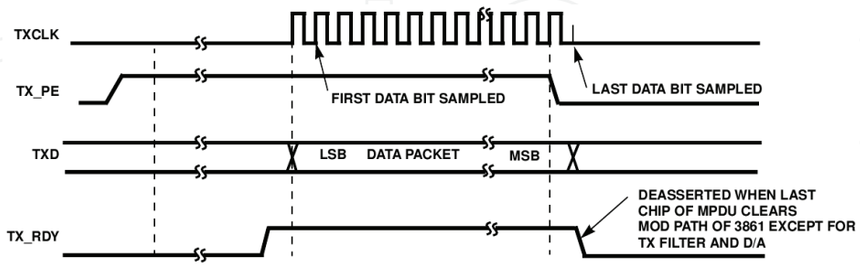

(a) Tx port timing

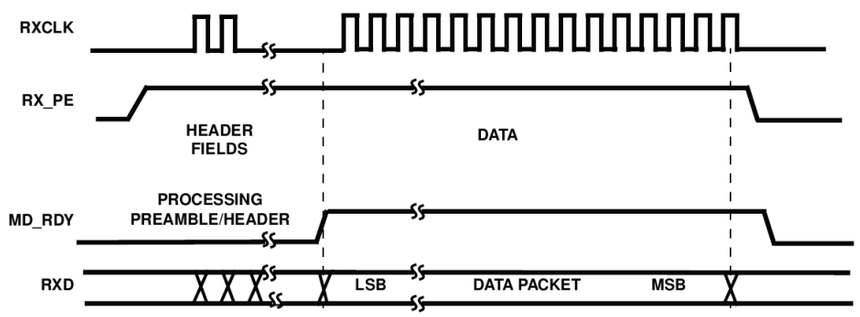

(b) Rx port timing

Fig. 2. Timing behavior of *TX_RDY* and *MD_RDY* signals.

If we access the physical layer of the WLAN adapter, we lose the control of what instant corresponds with which frame sent or received. That is way we access the interface between the physical and MAC layers of the WLAN adapter. This way, it will be easy to associate transmission times and reception times with sent and received frames, respectively. Among the commercial chip sets that work as interface between the physical and MAC layers, the Intersil HFA3861B baseband processor is fully free documented (Intersil, 2002).

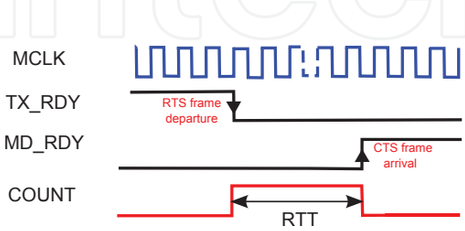

(a) RTT

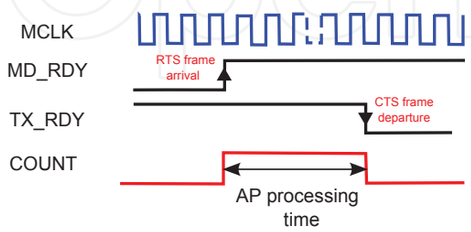

(b) AP processing time

Fig. 3. Timing diagram to mesure the RTT and the processing time of the AP.

From an inspection of the Intersil HFA3861B component pinout diagram, three appropriate leads (and common ground) were identified, *TX_RDY*, *MD_RDY* and *MCLK* (Intersil, 2002).

TX_RDY is an output of the external network processor indicating that preamble and header information has been generated and that the HFA3861B is ready to receive the data packet from the network processor over the *TXD* serial bus (see Fig. 2(a)). *MD_RDY* is an output signal of the network processor, indicating that header data and a data packet are ready to be transferred to the processor (see Fig. 2(b)). *MCLK* is the 44 MHz master clock that governs MAC layer processing. In Fig. 2(a) and 2(b) *TXCLK* and *RXCLK* clocks govern the signals *TX_RDY* and *MD_RDY*, respectively. These signals, *TXCLK* and *RXCLK*, are generated through the master clock *MCLK*. Therefore, as *TX_RDY* and *MD_RDY* signals are synchronized with *TXCLK* and *RXCLK*, respectively, they will be also synchronized with the master clock, *MCLK*.

Thus, in case the RTT is measured, the falling edge of the *TX_RDY* signal is used to start the counter (RTS frame departure) and the rising edge of the *MD_RDY* signal is used to stop it (CTS frame arrival). If the processing time of the AP is wanted to be measured, the rising edge of the *MD_RDY* signal is used to start the counter (RTS frame arrival) and the falling edge of the *TX_RDY* signal is used to stop it (CTS frame departure).

To quantify the RTT a 16-bit counter is used as measuring system and its input is the aforementioned *MCLK* lead, which allows to measure times up to 1.489 ms (2^{16} *MCLK* cycles). The triggers of the counter will be the *TX_RDY* and *MD_RDY* leads. As these triggers are *MCLK* synchronized, the count accuracy will not improve although a higher clock frequency was used.

The counter is integrated in a PCB (see Fig. 4). The PCB is made up of four serial 4-bit counter resulting in a 16-bit counter; one Flip-Flop and one XOR gate to form the RTT signal, managing the *TX_RDY* and *MD_RDY* triggers so that the RTS and CTS frames can be used as triggers to start and stop the measuring system; three 4-bit multiplexers to read the state of the four 4-bit counters; and the corresponding bypass capacitors between power supply and common ground to speed up the PCB commutation times, and to form a low pass filter which will prevent from high frequency disruptions. With the aim of reducing the loop area both for the supply and the signal tracks, top and bottom planes of the PCB were poured of copper, one attached to the power supply lead and the other attached to the common ground. This will minimize the impedance of the return path. In order to control the measuring system, the PCB is governed by the MS through the universal serial bus (USB) port.

The PCB measures the RTT as follows:

1. The MS enables the counters prior to send the RTS frame.
2. The last bit of the sending RTS frame starts the counters.
3. The first bit of the receiving CTS frame stops the counters.
4. Once the RTS/CTS two-frame exchange is completed the MS disables the counters.
5. The MS saves the state of the four 4-bit counters through the multiplexers.

The measuring system proposed has some limitations. First of all, as the *MCLK* that governs the PCB is 44 MHz frequency, the 16-bit counter implemented on the PCB cannot measure RTTs over 1.489 ms, but this time is enough for wireless networks range. Secondly, as a frame coming from other wireless nodes could activate or deactivate the count within the short lapse of time in which the measuring system is enabled, a filter that rejects these undesirable measurements is implemented. Filter limits have been chosen based on previous trials where there were no other wireless nodes interfering. Finally, according to (Bahillo et al., 2009) the elapsed time in the AP, between receiving a RTS frame and sending the corresponding CTS frame, can be assumed to be constant when there are no other processes competing for the AP

resources. Obviously, although the CTS frame has the highest priority (Gast, 2002), it could be concurrent RTS frames coming from other MS at the same AP increasing the load of the AP. In that case, if there are not enough APs in range to apply the localization algorithm, the wireless localization system delay increases, but the accuracy is not degraded thanks to the previous filter that rejects the RTT measurements that are out of the expected range.

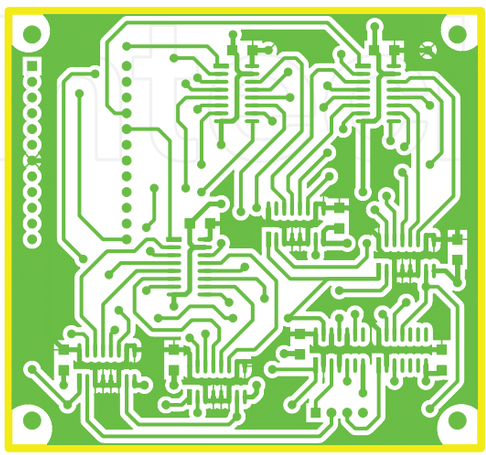

(a) Top layer

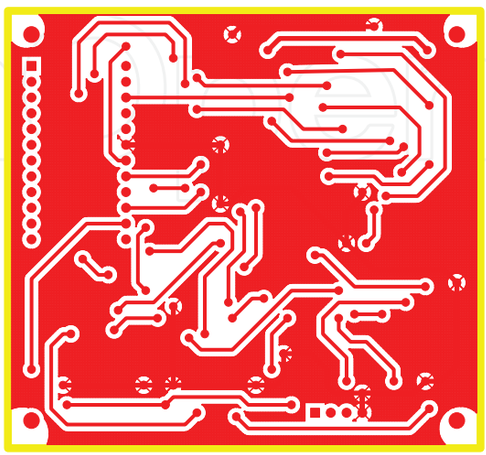

(b) Bottom layer

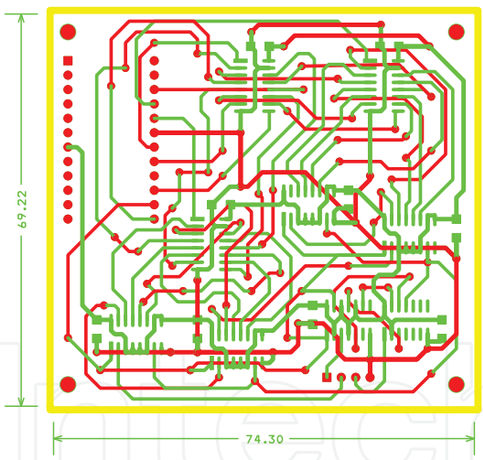

(c) Layer connections

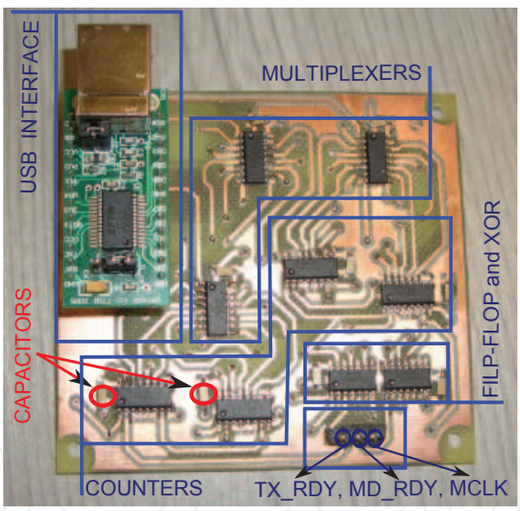

(d) Printed circuit board

Fig. 4. Printed Circuit Board, 69×74 [mm^2] size, used to measure the RTS/CTS two-frame exchange.

Regardless of the PCB size, the core of the measuring system is the counter, because the other components have to control the measuring system. If the measuring system would be integrated in the WLAN adapter, only the counter component and the driver to control it would be needed.

2.2 Experimental validation

After using the circuit simulation software *Pspice* to check that the PCB design works as expected, it is necessary to check that the PCB connected to the WLAN adapter and managed by the MS is able to measure the time delay when interchanging RTS/CTS frames.
The wireless devices involved in the experimental validation can be found in most wireless networks. They are:

1. A MS, an 802.11b wireless cardbus adapter, specifically a Cisco Aironet AIR-PCM340 with the HFA3861B baseband processor. The wireless adapter has been connected to the computer through a cardbus extender to be able to access to the HFA3861B pinout. This wireless adapter includes two on-board patch antennas with a diversity switch which toggles to and from, and stops when a significant amount of radio frequency power is detected.
2. An AP, a Linksys WRT54GL 802.11b/g. This AP includes two rubber duck omnidirectional antennas in diversity mode that never work at the same time, since diversity circuitry switches to the one with better reception. Rubber duck antennas provide vertical polarization with 360 degrees of coverage in the horizontal plane and 75 degrees in the vertical one. The AP was configured to send a beacon frame each 100 ms at constant power on 802.11 frequency channel 1 (2.412 GHz).

Using these wireless devices, several measurement campaigns were carried out in two different scenarios: an esplanade with a few streetlamps and trees, in the following *exterior*; and the corridor of a building $50 \times 4.3 \times 3.5$ m^3 (length, width and hight) size with wooden and metal doors and a few people walking around, in the following *corridor*. In all scenarios, the two WLAN devices which were involved in the scheme of the experimental setup were always in line-of-sight on a cardboard box 1.5 m high each, in order to guarantee the first Fresnel zone clearance.

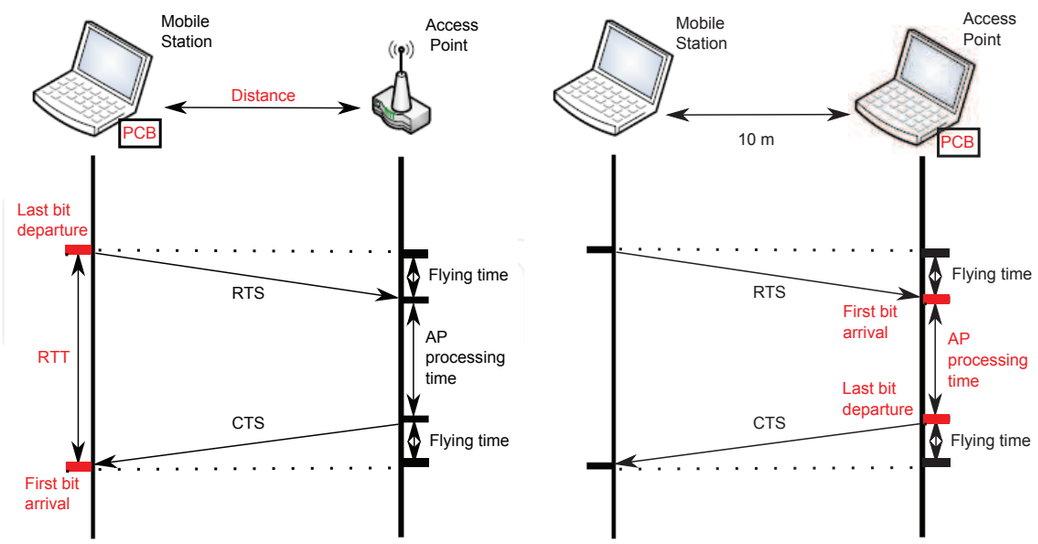

(a) RTT (b) AP processing time

Fig. 5. Experimental setup.

As shown in Fig. 5(a), in case the RTT is measured, the last bit of the RTS frame departure is used to start the counter and the first bit of the CTS frame arrival is used to stop it. If the processing time of the AP is wanted to be measured (see Fig. 5(b)), the first bit of the RTS frame arrival is used to start the counter and the last bit of the CTS frame departure is used to stop it.

2.2.1 RTT measurements

RTT measurements were performed using one Cisco WLAN adapter acting as a MS and one Linksys WRT54GL acting as an AP. The PCB was connected to the WLAN adapter of the MS. Three campaigns of 5000 RTT measurements were conducted at each position for several distances from 0 to 40 m.

Fig. 6 shows the RTT measurements obtained in terms of the number of *MCLK* cycles elapsed at each distance and environment, *exterior* and *corridor*. Each mark in Fig. 6 represents the mean of each group of 150 RTT measurements. The result is qualitatively consistent because, as it was expected, the delay profile observed shifts to the right as the actual distance between the two WLAN nodes increases, and it follows a linear form.

As Fig. 6 shows, although a direct path exists between the MS and the AP in all scenarios and distances, the delay profile observed is spread around 4 *MCLK* cycles. Besides the random behavior of the electronics, there are two main reasons: first of all, the frequency clock that governs the MS and the AP is 44 MHz and 20 MHz, respectively. Secondly, because of the multipath and the scatters of the environment, the direct path is not always the one selected by WLAN adapters. Therefore, to estimate the distance between the MS and the AP, a statistical estimator of the delay profile observed has to be selected. It will be discussed in the following section.

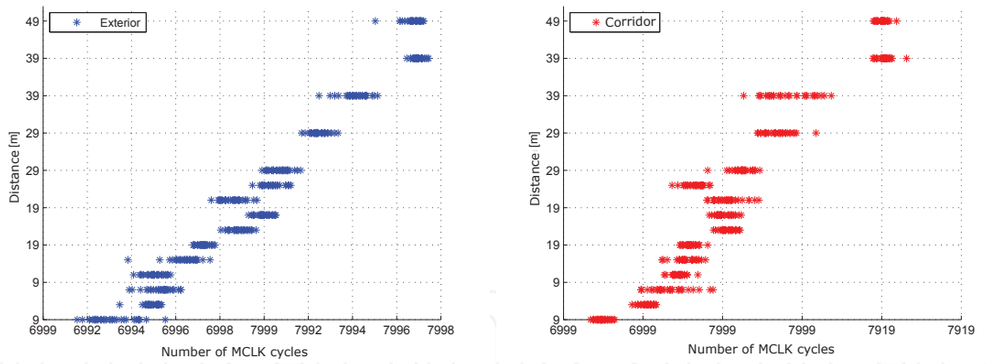

(a) Exterior (b) Corridor

Fig. 6. RTT measurements between two WLAN nodes in LOS at different distances in two different scenarios, *exterior* and *corridor*.

2.2.2 AP processing time measurements

The AP processing time is measured in the two scenarios described above (*exterior* and *corridor*) in order to check that the AP processing time is constant when the RTS/CTS two frame exchange is performed. As the WLAN MAC chip set of the Linksys WRT54GL 802.11b/g is not for public access, in this section the Cisco AIR-PCM340 WLAN adapter is used in AP mode. Therefore, a testing for this AP processing time approach was performed

using two Cisco WLAN adapters, one acting as a MS and the other acting as an AP. The PCB was in the AP. By using a driver designed by ourselves, based on the LORCON library, the MS sends a RTS frame to the AP identified through the MAC address and it waits for the corresponding CTS frame response. When the AP processing time is measured, the measuring system was not disabled between two RTS/CTS frames exchange because the AP does not know, a priori, the time the RTS frames arrival because they are not synchronized. As other frames coming from other WLANs could start or finish the count, the AP processing time measurements have to be filtered a posteriori, because the triggers that starts and finishes the count could not match with our RTS/CTS frames exchange.
As the AP processing time is independent of distance, the measurements were conducted for a distance of 10 m between the two WLAN adapters in the two scenarios, *exterior* and *corridor*.

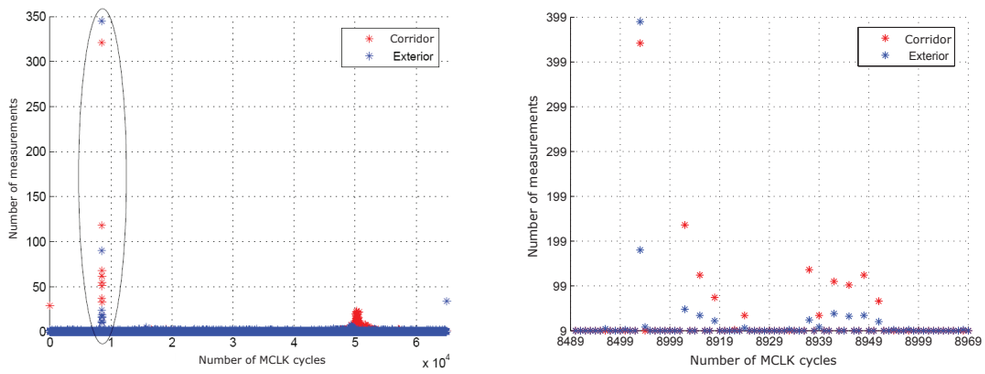

(a) Zoom out (b) Zoom in

Fig. 7. AP processing time measurements in two different scenarios, *exterior* and *corridor*.

As Fig. 7 shows, there are mainly four different behaviors about AP processing time measurements, which are around 0, 8500, 50000 and 65000 *MCLK* cycles. The extreme values, 0 and 65535 *MCLK* cycles, mean that the measuring system has not started the count before reading the counters state and the count has overflow, respectively. Measurements around 50000 *MCLK* cycles are not due to the RTS/CTS frame exchange because this behavior does not appear in the *exterior* environment, where there were not signals coming from other 802.11 devices. Measurements around 8500 *MCLK* cycles do not appear when the MS does not send the RTS frames. Therefore, these measurements, around 8500 *MCLK* cycles, are due to the AP processing time. When a RTS/CTS frame exchange is performed, it is assumed that the AP processing time is roughly constant because more than 50% of measurements, which are around 8500 *MCLK* cycles, were exactly 8494 *MCLK* cycles, although this actual value of the AP processing time is not needed to apply the ranging method we propose in next section.

3. Distance estimation in LOS

According to (Chen & Ling, 2002), the range resolution is determined by the bandwidth of the transmitted signal when RTT measurements are used. High-precision location would require large transmission bandwidths or the use of multiple frequency channels. Furthermore, when using a 44 MHz clock as input of the measuring system to quantify the RTT measurements, the maximum resolution achievable, if only one sample is taken, is hampered by that frequency clock. Moreover, even in a LOS environment the RTT measurements have a random behavior

due to the error introduced by the standard noise from electronic devices, that is always present. Therefore, to overcome these limitations several RTT measurements have to be performed at each distance and a representative value, called the location estimator, from this group of RTT measurements has to be selected as the distance estimation. The selection of the location estimator is based on the model that relates the location estimator to the distance that separates the MS and the AP.

The location of a random variable distribution can usually be presented by a single number, the location estimator. In (Olive, 2008), several location estimators of a random variable are analyzed. The mean, median, mode and the scale parameter of the Weibull distribution (scale-W) are examples of the location of a random variable. In this chapter, they have been analyzed and compared as location estimators of the RTT measurements in terms of the coefficient of determination, r^2. This coefficient measures how much of the original uncertainty in the RTT measurements is explained by the model (Weisberg, 2005). In this chapter, a simple linear regression function is assumed to be the model that relates the actual distance between the two wireless nodes involved in RTT measurements to the location estimators in LOS.

Analytically,

$$\widehat{d}_{RTT}^{LOS} = \beta_0 + \widehat{RTT}\beta_1 = d + \epsilon_{LOS}, \tag{1}$$

where, $\widehat{d}_{RTT}^{LOS}$ and d are the estimated and the actual distance between the MS and the AP in LOS, respectively, $\widehat{RTT}$ is the location estimator of RTT measurements, β_0 and β_1 are the intercept and slope of the simple linear regression function, respectively, and ϵ_{LOS} is the error introduced by $\widehat{RTT}$. The error term ϵ_{LOS} has been modeled as a zero-mean Gaussian random variable, because the estimators used are asymptotically Gaussian and a large amount of measurements have been used, so

$$\epsilon_{LOS} \rightsquigarrow N(0, \sigma_{LOS}). \tag{2}$$

In this case, as the expression (1) is a simple linear regression function, r^2 is simply the square of the correlation coefficient, $r^2_{\widehat{RTT},d}$.

The parameters β_0 and β_1 that characterize the simple linear regression function do not depend on the environment where the wireless localization system is going to be deployed, but on the communication system used, i.e. the MS and the AP. These parameters are computed so as to give a best fit of the location estimators to the actual distance. Most commonly, the best fit is evaluated by using the least squares method, but this method is actually not robust in the sense of outlier-resistance. Hence, robust regression has been performed as it is a form of regression analysis designed to circumvent some limitations of least squares estimates for regression models (Olive, 2008).

Assuming LOS between the MS and the AP without any scatter nearby and guaranteeing the first Fresnel zone clearance of the link between both nodes, three campaigns of RTT measurements were conducted for several distances from 0 to 40 m. Fig.8 shows the robust linear regression function which best fits each location estimator to be analyzed. Each location estimator has been computed from each group of 150 RTT measurements at each distance. The different location estimators are analyzed and compared in terms of the coefficient of determination value, r^2.

The mode ($\widehat{RTT}_{md}$) is the value that is most likely to be sampled, thereby it could be a good candidate for the location estimator, but the value that occurs the most frequently in a data

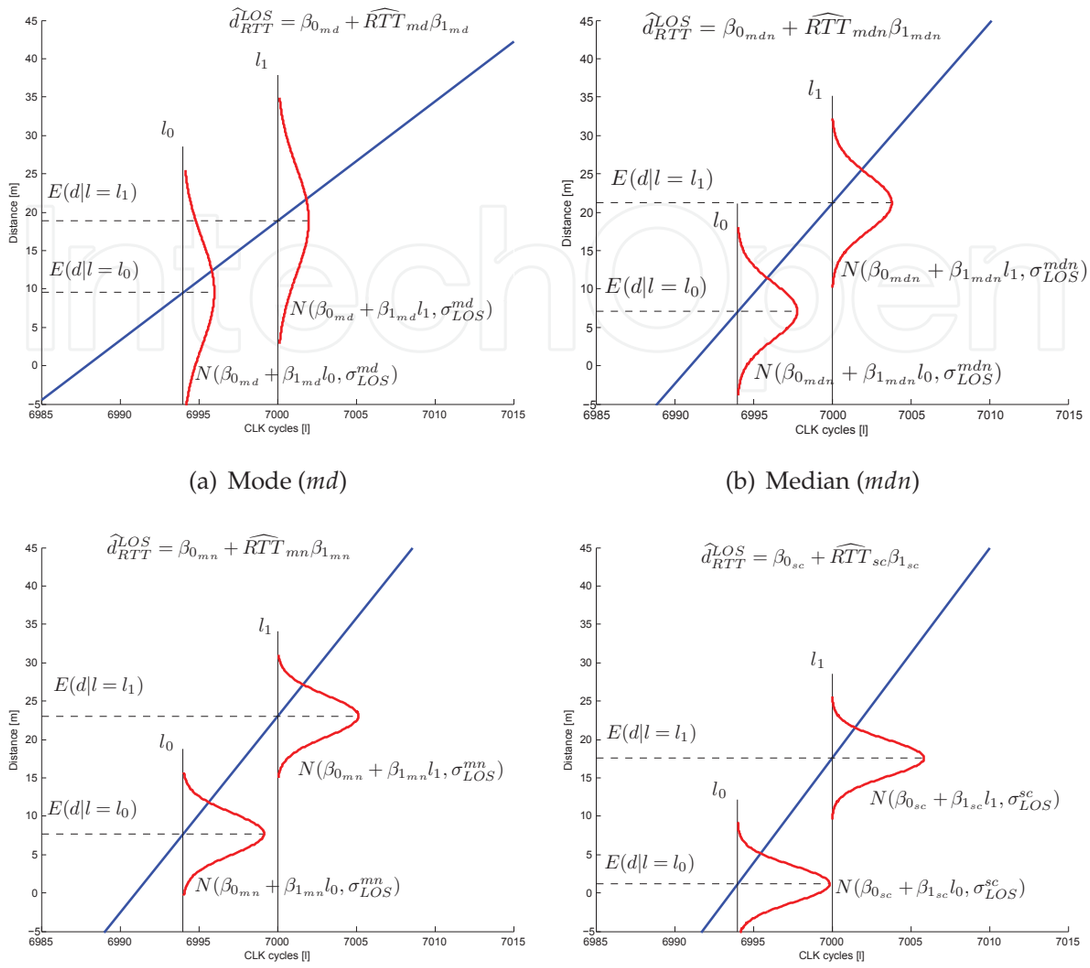

(a) Mode (*md*) (b) Median (*mdn*)

(c) Mean (*mn*) (d) Scale-W (*sc*)

Fig. 8. Robust linear regression function that best fits each location estimator to be analyzed: the mean, median, mode and scale-W parameter. Where each location estimator is computed from groups of 150 RTT measurements at each distance.

set is a discrete value. Therefore, the resolution achieved, T_{MCLK}, is not enough for indoor localization systems. The same resolution is achieved with the median ($\widehat{RTT}_{mdn}$) as it is a discrete value separating the higher half of a data set. Fig.8 (a) (b) show that the Gaussian distributions that characterize the errors ϵ_{LOS} of the mode and the median are the widest, $\sigma_{LOS}^{md} = 7$ m being $r_{md}^2 = 0.64$ and $\sigma_{LOS}^{mdn} = 3.6$ m being $r_{mdn}^2 = 0.9$.

The mean ($\widehat{RTT}_{mn}$) is equivalent to the center of gravity of the distribution and it does not take discrete values, thereby the resolution is improved. Although the mean is rather sensitive in the presence of outliers, the use of a robust regression function circumvents this limitation. Fig.8 (c) shows the errors committed when using the mean as location estimator are characterized by a Gaussian, $\sigma_{LOS}^{mn} = 2.7$ m, being $r_{mn}^2 = 0.94$, lower than the error commit when the median. However, Fig.8 (d) shows that the best location estimator is the

scale-W parameter ($\widehat{RTT}_{sc}$) once Weibull distribution is fitted to the RTT measurements. In this case ϵ_{LOS} is characterized by $\sigma^{sc}_{LOS} = 2.3$ m and $r^2_{sc} = 0.96$. Therefore, the assumption of a linear function as the model that relates RTT measurements to distance is corroborated by a correlation coefficient value close to the unit. This value indicates that the regression line nearly fits the $\widehat{RTT}_{sc}$ perfectly.
There is no phenomenological explanation for choosing the scale-W parameter as location estimator of the RTT measurements set, however this parameter is another kind of a location estimator since the maximum likelihood estimator (MLE) of the scale-W parameter is the Hölder mean (Borwein & Borwein, 1986), a generalized form of the Pythagorean means, taking as parameter the shape parameter of Weibull distribution (for more detail see appendix).

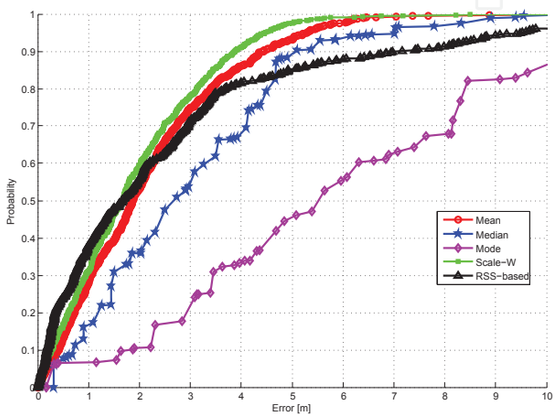

Fig. 9. CDFs of distance errors performed with four different location estimators and a RSS-based method.

Once scale-W parameter is found as the statistical estimator of the RTT measurements that best fits the actual distance when using a simple robust linear regression function as the model that relates the estimator to the distance, its performance is compared to a RSS-based solution to evaluate the goodness of the proposed one. The same two wireless nodes have been used in the same LOS environment. As it is well known the distance between two wireless devices causes an attenuation in the RSS values. This attenuation is known as path-loss and it is modeled to be inversely proportional to the distance between both devices raised to a certain exponent. According to (Mazuelas et al., 2009), the distance between two wireless nodes can be estimated from RSS measurements by

$$\widehat{d}_{RSS} = 10^{\frac{P_{ref} - \overline{P}}{10\alpha}} \tag{3}$$

where $\widehat{d}_{RSS}$ is the estimated distance between the MS and the AP, P_{ref} is the RSS measured in logarithmic units at the reference distance of 1 m, $\overline{P}$ is the average RSS in logarithmic units at the actual distance, and α is the path-loss exponent. According to (IEEE Standard, 2007), for any distance under 20 m in LOS, α is recommended to be 2 while $\alpha = 3.5$ for longer distances. Therefore, having taken this value for the path-loss exponent and from the RSS values measured between both devices, the distance between the two wireless nodes can be estimated by using the expression (3).
Fig.9 shows the cumulative distribution function (CDF) of distance errors. As the mode and the median take discrete values, the CDF has a step-shape with large errors. The mean has a

good behavior with an error lower than 2 m on average. However, the scale-W parameter with an error lower than 3 m for a cumulative probability of 80% achieves the best behavior. Also in Fig.9 it can be appreciated that the scale-W parameter outperforms the RSS range based method, specially for cumulative probabilities larger than 50%.

4. Distance estimation in NLOS

The assumption that LOS propagation conditions are present in an indoor environment is an oversimplification of reality. In such environments the transmitted signal could only reach the receiver through reflected, transmitted, diffracted, or scattered paths. Hence, these paths could positively bias the actual distance caused mainly by the blocking of the direct path or due to experiencing a lower propagation speed through obstacles (Allen et al., 2007).
Known as the NLOS problem, this positive bias has been deeply considered through the literature with the aim of mitigating its effect on distance estimates (Mazuelas et al., 2008; Tang et al., 2008; Wylie & Holtzman, 1996), however, in all of them the NLOS is mainly discussed within the cellular networks. Note that such techniques usually assume that the bias for the NLOS range measurements changes over time and has larger variances than LOS range measurements (Güvenç et al., 2008), assumptions that could not be assured in an indoor environment (Yarkoni & Blaunstein, 2006).
In an indoor environment, the easiest method for dealing with NLOS conditions is simply to place APs at additional locations and select those from LOS, however one of the objectives of this chapter is to deploy a wireless localization system in a common and unmodified wireless network. Therefore, in this chapter, the feasibility of the PNMC method presented in (Mazuelas et al., 2008) is analyzed in an indoor environment, taking the PCB proposed in previous section as measuring system, the scale-W as statistical estimator of the RTT and the simple linear regression as the model to relate the scale-W to the actual distance.
The PNMC method relies on the statistical distribution of NLOS errors and on the major variance that NLOS errors present with respect to LOS. The distribution type of NLOS errors depends on the particular environment. Hence, it can follow different statistical distributions such as Gaussian, Exponential, Gamma, etc. (Mazuelas et al., 2008). Regarding the distribution, its parameters can be assumed to be constant in that particular environment. Moreover, those parameters can be obtained before the process of getting distance estimates (Cong & Zhuang, 2005) or directly from the estimated delay spread at that moment (Urrela et al., 2006). In this chapter, those parameters have been obtained beforehand by a campaign of RTT measurements in NLOS.
Let d be the actual distance between the MS and the AP, thus

$$\widehat{d}_{RTT}^{NLOS} = d + \epsilon, \tag{4}$$

where, $\widehat{d}_{RTT}^{NLOS}$ and d are the estimated and the actual distance between the MS and the AP, respectively. The term ϵ denotes the error in the estimation of the distance. This error is the sum of two independent errors, $\epsilon = \epsilon_{LOS} + \epsilon_{NLOS}$, where ϵ_{LOS} describes the noise form electronic errors, while ϵ_{NLOS} is the error due to the lack of direct sight between the MS and the AP. On the one hand, the term ϵ_{LOS} has been evaluated in the previous section and it was found as a zero-mean Gaussian with $\sigma_{LOS} = 2.3$ m. On the other hand, the term ϵ_{NLOS} can follow different statistical distributions. However, regarding the distribution of ϵ_{NLOS}, it can be characterized by its mean and standard deviation. These parameters, as well as the distribution type of ϵ_{NLOS}, depends on the particular environment, but it can be assumed

that the NLOS propagation conditions do not change significantly in the time window that contains the record of range measurements, so the mean and standard deviation of ϵ_{NLOS} can be assumed to be constant. Moreover, the parameters that characterize ϵ_{NLOS} can be obtained previously to the localization process by the estimates performed in the environment where the localization system is going to be deployed. For simplicity, the Exponential distribution has been chosen for the term ϵ_{NLOS}. Therefore,

$$\epsilon_{NLOS} \rightsquigarrow Exponential(\lambda) \tag{5}$$

where the λ parameter is fixed previously to the localization process.

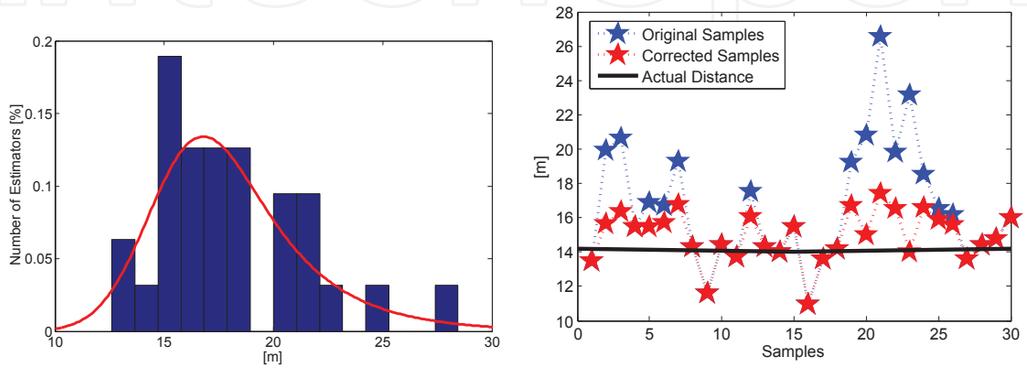

(a) Histogram (b) Estimators

Fig. 10. NLOS error correction from a record of distance estimates. (a) Histogram of distance estimates and the probability density function that best fits the data. (b) Record of original and corrected distance estimates after having applied the PNMC method.

In order to show the feasibility of the PNMC technique in an indoor environment, a campaign of measurements in the second floor of the Higher Technical School of Telecommunications Engineering (ETSIT) at the University of Valladolid has been carried out. Specifically, the PNMC technique is applied to the range measurements computed between an AP and a MS 14 m away who is moving 5 m straight perpendicularly to the path that joins the AP and the MS. As $\epsilon = \epsilon_{LOS} + \epsilon_{NLOS}$, the probability density function (PDF) of the term ϵ is the convolution of the Gaussian PDF caused by the ϵ_{LOS} errors and the Exponential PDF caused by the ϵ_{NLOS} errors. Fig.10 (a) shows the histogram of the distance estimates record and the PDF of the term ϵ that best fits these estimates, where the value of the parameter λ that best fits the data is $\lambda = 0.3$ m^{-1}. Once the term ϵ is statistically characterized, the PNMC technique can be applied. Fig.10 (b) shows the result of applying the PNMC technique to the original range measurements computed in a time window equivalent to 5 m walking. In this scenario, the ratio of ϵ_{NLOS} errors from the record of range measurements has been 52%. Subsequently, these NLOS range measurements have been corrected by subtracting the expected NLOS errors for each segment according to the Exponential distribution.

5. Experimental validation

The second floor of the ETSIT as a real indoor environment with several offices, rooms and many people walking around has been the selected scenario to test the wireless localization

system's accuracy. The 802.11 wireless network deployed in that building has been used as the one over which the MS communicates with their APs whose positions are previously known. Fig. 11 shows the layout of the south-wets of the second floor of the ETSIT building where positioning tests have been carried out. The route followed by the MS describes a 40×11 m^2 rectangle walking through the middle of the corridors where each pair of continuous positions is separated 0.75 m approximately. The corridors involved in the route are 2 m wide except the widest one that has a width of 4.3 m. As a consequence of the heterogeneous distribution of rooms and offices, and the people walking around, multiple reflection, diffraction or scatter points could appear and alter the signal path. Presumably, although NLOS is always present, multipath will be more noticeable when moving along the narrowest corridors.

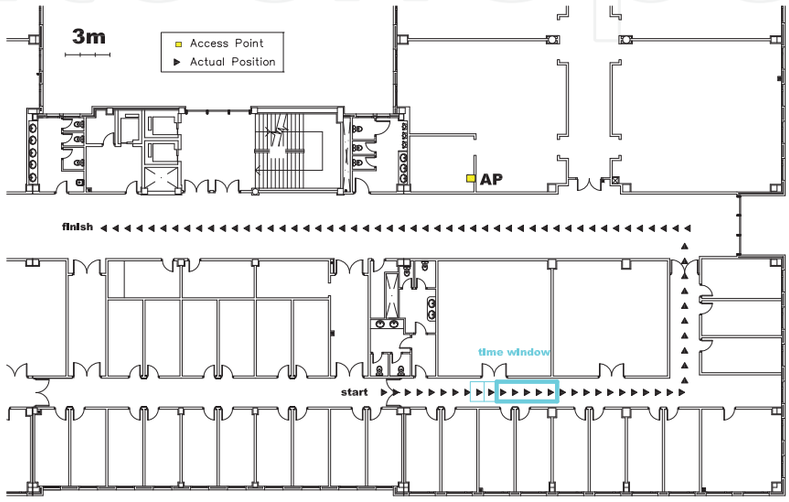

Fig. 11. Indoor environment where RTT measurements have been carried out.

RTT measurements have been performed between an AP fixed in a laboratory and a MS which was moving on the route shown. Any of the positions on the route has a direct sight to the AP, situation that could possibly happen in any indoor environment with high probability. Therefore, the route followed shows different degrees of NLOS instead of LOS and NLOS combinations.

The error introduced by the term NLOS is corrected by using the PNMC technique, where NLOS is observed to be exponentially distributed with λ =0.3 m^{-1} and a time window equivalent to 5 m walking is used. As location estimator, the scale-W parameter has been implemented to reduce the error produced by the term LOS.

Fig. 12(a) shows the actual distance from the MS to the AP at each position through the route shown in Fig. 11. The distance estimate, in red, at each position is shown by using the scale-W as statistical estimator of the RTT, having applied the linear regression model. As it is observed in Fig. 12(a), due to the fact that the positions where the MS is going to be located do not have a direct sight to the AP, the distance estimates are almost always higher than the actual one. Therefore, PNMC method is going to correct distance estimates with severe NLOS. In blue, the distance estimates having applied the PNMC method on the computed distance estimates are shown. They are more similar to those that would be obtained in the absence of severe NLOS propagation.

It can be concluded that although the difference between σ_{LOS} and σ_{NLOS} is not so great, the presence of severe NLOS in the record is detected and corrected. As it is shown in

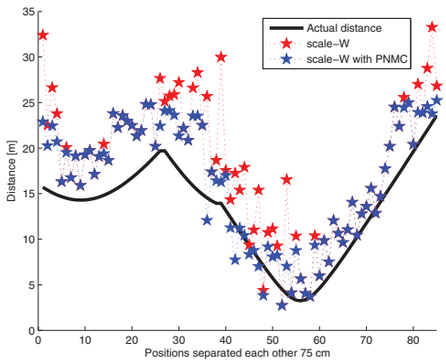

(a) Correction of severe NLOS measurements with PNMC

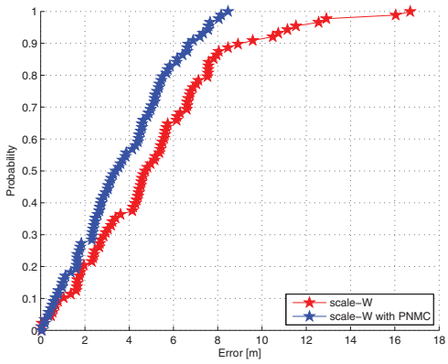

(b) CDF

Fig. 12. NLOS error mitigation from a record of distance estimates using a window size of 5 m walking. (a)scale-W distance estimates before and after applying PNMC method. (b) Comparison of CDFs errors in distance estimate before and after applying PNMC method.

Fig. 12(b) the improvement of applying the PNMC method can be observed through the CDF of errors in distance estimates. Generally speaking, the distance estimate can be improved on approximately 2 m for cumulative probabilities higher than 30% when applying the PNMC method.

6. Conclusions

The achievable positioning accuracy of traditional wireless localization systems is limited when harsh radio propagation conditions like rich multipath indoor environments are present. In this chapter a novel RTT-based ranging method is proposed over a PCB that performs RTT measurements. The effect of hardware errors has been minimized by choosing the scale-W parameter as RTT estimator. A coefficient of determination value of 0.96 achieved with this estimator in LOS justified the simple linear regression function as the model that relates distance estimates to RTT measurements in LOS. As LOS is not guaranteed in an indoor environment, the accuracy of the proposed localization algorithm has been tested in a rich multipath environment without any NLOS error mitigation technique achieving an error lower than 4 m on average. However, this error is improved after having implemented the PNMC technique to correct NLOS errors. Once reliable RTT-based ranging estimates are obtained, simple geometrical triangulation methods can be used to find the location of the MS (Pahlavan & Krishnamurthy, 2002).

Indoor localization schemes have experienced a flurry of research in recent years. However, there still remain multiple areas of open research that will help systems to meet the requirements of applications that have to operate in indoor propagation environments where GNSS typically fails. These are: i) Interference mitigation: To date, the majority of research effort ignores the effects of interference on time estimation accuracy, and few papers propose robust interference mitigation techniques. ii) Inertial Measurements Units (IMU): the integration of traditional localization metrics, such as TOA, RSS or AOA with IMU information, such as the one reported by accelerometers, gyroscopes and magnetometers, could provide location estimations more precisely and continuously, since IMU-based

localization is a beacon-free methodology. iii) Secure ranging: In certain scenarios the localization process may be subject to hostile attacks. While some works have presented secure localization algorithms (see, e.g., (Li et al., 2005; Zhang et al., 2006)), less attention has been paid to secure ranging.

7. Acknowledgment

This research is partially supported by the General Board of Telecommunications of the Council of Public Works from Castilla-León (Spain) and by the spanish national project LEMUR (TIN2009-14114-C04-03).

8. Appendix

8.1 Maximum likelihood estimator of the scale parameter of the Weibull distribution

The scale-W parameter is estimated by using the MLE method and assuming that the shape parameter is known.
The probability density function of a Weibull (two-parameter) random variable x is

$$\begin{aligned} f(x;k,\lambda) &= \frac{k}{\lambda}\left(\frac{x}{\lambda}\right)^{k-1}\cdot e^{-\left(\frac{x}{\lambda}\right)^k} \qquad x \geq 0 \\ &= \frac{k}{\lambda^k}\cdot x^{k-1}\cdot e^{-\left(\frac{x}{\lambda}\right)^k} \qquad x \geq 0 \end{aligned}$$

where $k > 0$ is the shape parameter and $\lambda > 0$ is the scale-W parameter.
Let $X_1, X_2, ...X_n$ be a random sample of random variables with two-parameter Weibull distribution, k and λ. The likelihood function is

$$L(x_1, ...x_n; k, \lambda) = \prod_{i=1}^{n} f(x_i; k, \lambda)$$

Therefore,

$$\begin{aligned} lnL(x_1, ..., x_n; k, \lambda) &= \sum_{i=1}^{n} lnf(x_1, ...x_n; k, \lambda) \\ &= \sum_{i=1}^{n}\left(ln\left(\frac{k}{\lambda}\right) + (k-1)\cdot ln\left(\frac{x_i}{\lambda}\right) - \left(\frac{x_i}{\lambda}\right)^k\right) \\ &= n\cdot ln\left(\frac{k}{\lambda}\right) + (k-1)\cdot\sum_{i=1}^{n} ln\left(\frac{x_i}{\lambda}\right) - \sum_{i=1}^{n}\left(\frac{x_i}{\lambda}\right)^k \\ &= n\cdot(ln(k) - ln(\lambda)) + (k-1)\cdot\left[-n\cdot ln(\lambda) + \sum_{i=1}^{n} ln(x_i)\right] - \sum_{i=1}^{n}\left(\frac{x_i}{\lambda}\right)^k \\ &= n\cdot ln(k) + (k-1)\cdot\sum_{i=1}^{n} ln(x_i) - n\cdot k\cdot ln(\lambda) - \lambda^{-k}\cdot\sum_{i=1}^{n} x_i^k \end{aligned}$$

thus,

$$\frac{\partial lnL}{\partial\lambda} = -n\cdot k\cdot\frac{1}{\lambda} + k\cdot\frac{1}{\lambda^{k+1}}\cdot\sum_{i=1}^{n} x_i^k$$

in order to find the maximum, $\frac{\partial lnL}{\partial \lambda} = 0$ then,

$$0 = -n \cdot k \cdot \frac{1}{\lambda} + k \cdot \frac{1}{\lambda^{k+1}} \cdot \sum_{i=1}^{n} x_i^k$$
$$= \frac{\sum_{i=1}^{n} x_i^k - n \cdot \lambda^k}{\lambda^{k+1}}$$
$$= \sum_{i=1}^{n} x_i^k - n \cdot \lambda^k$$

hence, the MLE of the scale-W parameter

$$\widehat{\lambda} = \left[\frac{1}{n} \sum_{i=1}^{n} x_i^k \right]^{\frac{1}{k}}$$

this expression is known as the generalized mean or Hölder mean.
The Hölder mean is a generalized mean of the form,

$$M_p(x_1, x_2, ..., x_n) = \left[\frac{1}{n} \sum_{i=1}^{n} x_i^p \right]^{1/p} \tag{6}$$

where the parameter p is an affinely extended real number, n is the number of samples and x_i are the samples with $x_i \geq 0$. The Hölder mean is an abstraction of the Pythagorean means which for example includes minimum ($M_{-\infty}$), harmonic mean (M_{-1}), geometric mean (M_0), arithmetic mean (M_1), quadratic mean (M_2), maximum (M_{∞}), and the MLE of the scale-W parameter (M_k) where k is the shape parameter of Weibull distribution.

9. References

Bahillo, A., Mazuelas, S., Lorenzo, R.M., Fernández, P., Prieto, J. & Abril, E.J. (2009a). Indoor location based on IEEE 802.11 round-trip time measurements with two-step NLOS mitigation. *Progress In Electromagnetics Research B, PIERB*, Vol.2009, No.15, (September 2009) 285-306, ISSN: 1937-6472.

Bahillo, A., Prieto, J., Mazuelas, S., Lorenzo, R.M., Blas, J. & Fernández, P. (2009b). IEEE 802.11 distance estimation based on RTS/CTS two-frame exchange mechanism, *Proceedings of 69th international conference of Vehicular Technologies*, pp. 1-5, ISBN: 978-1-4244-2517-4, Barcelona, June 2009, IEEE VTC, Spain.

Golden, S.A. & Bateman, S.S. (2007). Sensor measurements for wifi location with emphasis on time-of-arrival ranging. *IEEE Transactions on Mobile Computing*, Vol.6, No.10, (October 2007) 1185-1198, ISSN: 1536-1233.

Gustafsson, F. & Gunnarson, F. (2005). Mobile positioning using wireless networks: possibilities and fundamental limitations based on available wireless network measurements. *IEEE Signal Processing Magazine*, Vol.22, No.4, (July 2005) 41-53, ISSN: 1053-5888.

Mazuelas, S., Bahillo, A., Lorenzo, R. M., Fernández, P., Lago, F.A., García, E., Blas, J. & Abril, E. J. (2009). Robust indoor positioning provided by real-time RSSI values in unmodified WLAN networks. *IEEE Journal of Selected Topics in Signal Processing*, Vol.3, No.5, (October 2009) 821-831, ISSN: 1932-4553.

Mazuelas, S., Lago, F.A., Blas, J., Bahillo, A., Fernández, P., Lorenzo, R. M. & Abril, E. J. (2008). Prior NLOS measurements correction for positioning in cellular networks. *IEEE Transactions on Vehicular Technologies*, Vol.58, No.5, (November 2008) 2585-2591, ISSN: 0018-9545.

Morrison, J.D. (2002). IEEE 802.11 wireless local area network security through location authentication. *M.S. Thesis, Naval Postgraduate School Monterey, California.*

Pahlavan, K. & Krishnamurthy, P. (2002). *Principles of wireless networks - A unified approach*, Prentice-Hall Inc., 2nd edition, ISBN: 0-13-093003-2, Upper Saddle River, New Jersey.

Prieto, J., Bahillo, A., Mazuelas, S., Blas, J., Fernández, P. & Lorenzo, R. M. (2008). RTS/CTS mechanism with IEEE 802.11 for indoor location, *Proceedings of the Navigation Conference & Exhibition: Navigation and Location*, pp. 1-5, London, UK, October 2008, NAV & ILA.

Seow, C.K. & Tan, S.Y. (2008). Localization of omni-directional mobile device in multipath environments. *Progress In Electromagnetics Research, PIER*, Vol.85, No.2008, (2008), 323-348, ISSN: 1070-4698.

Soliman, M.S., Morimoto, T. & Kawasaki, Z.I. (2006). Three-dimensional localization system for impulsive noise sources using ultra-wideband digital interferometer technique. *Journal of Electromagnetic Waves and Applications*, Vol.20, No.4, (2006), 515-530, ISSN: 0920-5071.

Gast, M.S. (2002), *802.11 Wireless networks: the definitive guide*, O'Reilly & Associates, Inc., ISBN: 0-596-00183-5, 1005 Gravenstein Highway North, Sebastopol, CA 95472.

Chen, V.C. & Ling, H. (2002), *Time-frequency transforms for radar imaging and signal analysis*, Artech House, Inc., ISBN: 1-58053-288-8, 685 Canton Street, Norwood, MA, 02062.

Olive, D.J. (2008), *Applied robust statistics*, Southern Illinois University, Department of Mathematics, 4408 Carbondale, IL 62901-4408.

Weisberg, S. (2005), *Applied linear regression, 3rd ed.*, John Wiley & Sons, Inc., ISBN: 0-471-66379-4, Hoboken, New Jersey.

Intersil, (2002), *HFA3861B wireless LAN medium access controller*, Intersil Data Sheet.

Borwein, J.M. & Borwein, P.B. (1986), *Pi and the AGM: a study in analytic number theory and computational complexity*, John Wiley & Sons, Inc., ISBN: 0-471-83138-7, USA.

IEEE Standard for Information Technology (2007) *Telecommunications and Information Exchange Between Systems - Local and Metropolitan Area Networks - Specific Requirements - Part 11: Wireless Medium Access Control (MAC) and Physical Layer (PHY) Specifications, IEEE Std 802.11-2007 (Revision of IEEE Std 802.11-1999).*

Allen, B., Dohler, M., Okon, E., Malik, W., Brown, A. & Edwards, D., (2007), *Ultra Wideband Antennas and Propagation for Communications, Radar, and Imaging*, John Wiley & Sons, Inc., ISBN: 0-470-03255-3, West Sussex, UK.

Tang, H., Park, Y. & Qui, T., (2008). NLOS mitigation for TOA location based on a modified deterministic model. *Research Letters in Signal Processing*, Vol.8, No.1, (April 2008) 1-4, ISSN: 1687-6911.

Wylie, M. P. & Holtzman, J., (1996). The non-line of sight problem in mobile location estimation. *Proceedings of the 5th IEEE International Conference on Universal Personal Communications*, Vol.2, pp. 827-831, ISBN: 0-7803-3300-4, Cambridge, October 1996, Mass, USA.

Güvenç I., Chong, C.-C., Watanabe, F. & Inamura, H., (2008). NLOS identification and weighted least-squares localization for UWB systems using multipath channel

statistics, *EURASIP Journal on Advances in Signal Processing*, Vol. 2008, (April 2008) 1-14, ISSN: 1110-8657.

Yarkoni, N. & Blaunstein, N., (2006). Prediction of propagation characteristics in indoor radio communication environment. *Progress In Electromagnetics Research*, PIER 59, (2006) 151-174, ISSN: 1070-4698.

Cong, L. & Zhuang, W., (2005). Non-line-of-sight error mitigation in mobile location. *INFOCOM 2004, 23th Annual Joint Conference of the IEEE Computer and Communications Societies*, Vol. 4, pp. 560-572, ISBN: 0-7803-8355-9, Hong-Kong, March 2004.

Urrela, A., Sala, J. & Riba, J., (2006). Average performance analysis of circular and hyperbolic geolocation. *IEEE Transactions on Vehicular Technology*, Vol. 55, (January 2006) 52-66, ISSN: 0018-9545.

Chen, P.-C., (1999). A non-line-of-sight error mitigation algorithm in location estimation. *Proceedings of Wireless Communications and Networking Conference*, Vol. 1, pp. 316-320, ISBN: 0-7803-5668-3, New Orleans, La, USA, September 1999.

Li, Z., Trappe, W., Zhang, Y. & Nath, B., (2005). Robust statistical methods for securing wireless localization in sensor networks, *Proceedings of IEEE Information Processing Sensor Networks*, pp. 91-98, ISBN: 0-7803-9202-7, Los Angeles, California, USA, April 2005.

Zhang, Y., Liu, W., Lou, W. & Fang, Y., (2006). Location-based compromise-tolerant security mechanisms for wireless sensor networks, *IEEE Journal on Selected Areas in Communications*, Vol. 24, (February 2006) 247-260, ISSN: 0733-8716.

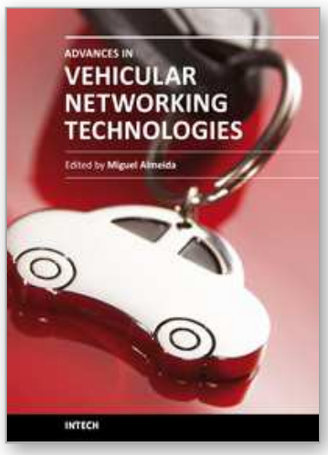

Advances in Vehicular Networking Technologies

Edited by Dr Miguel Almeida

ISBN 978-953-307-241-8
Hard cover, 432 pages
Publisher InTech
Published online 11, April, 2011
Published in print edition April, 2011

This book provides an insight on both the challenges and the technological solutions of several approaches, which allow connecting vehicles between each other and with the network. It underlines the trends on networking capabilities and their issues, further focusing on the MAC and Physical layer challenges. Ranging from the advances on radio access technologies to intelligent mechanisms deployed to enhance cooperative communications, cognitive radio and multiple antenna systems have been given particular highlight.

How to reference

In order to correctly reference this scholarly work, feel free to copy and paste the following:

Alfonso Bahillo, Patricia Fernández, Javier Prieto, Santiago Mazuelas, Rubén M. Lorenzo and Evaristo J. Abril (2011). Distance Estimation based on 802.11 RTS/CTS Mechanism for Indoor Localization, Advances in Vehicular Networking Technologies, Dr Miguel Almeida (Ed.), ISBN: 978-953-307-241-8, InTech, Available from: http://www.intechopen.com/books/advances-in-vehicular-networking-technologies/distance-estimation-based-on-802-11-rts-cts-mechanism-for-indoor-localization

INTECH
open science | open minds

InTech Europe
University Campus STeP Ri
Slavka Krautzeka 83/A
51000 Rijeka, Croatia
Phone: +385 (51) 770 447
Fax: +385 (51) 686 166
www.intechopen.com

InTech China
Unit 405, Office Block, Hotel Equatorial Shanghai
No.65, Yan An Road (West), Shanghai, 200040, China
中国上海市延安西路65号上海国际贵都大饭店办公楼405单元
Phone: +86-21-62489820
Fax: +86-21-62489821

IntechOpen